Complex Classical and Quantum Scattering Dynamics and the Quantum Hall Effect

S. A. Trugman
Theoretical Division, Los Alamos National Laboratory, Los Alamos, New Mexico 87545
(Received 20 October 1988)

The effect of a magnetic field on potential scattering is investigated microscopically. Analytic, exact renormalization-group, and numerical solutions show that the classical scattering dynamics of a charged particle is extremely complex. In one case, the dynamics is described by a discontinuous one-dimensional Hamiltonian map. Preliminary results indicate complex *quantum* dynamics as well. Consequences include an explanation of the observed breakdown of the quantum Hall effect at large currents and possible $1/f$ noise.

PACS numbers: 72.20.My, 05.45.+b, 72.70.+m, 73.40.Gk

The quantum Hall effect describes the transport of electrons in two dimensions in a magnetic field.[1] One of the most fundamental problems in the quantum Hall effect (QHE) is how potential scattering occurs in a magnetic field. This process is described by a scattering matrix $\langle\psi_{\rm out}|S|\psi_{\rm in}\rangle$, and is not in general understood. Much of the current understanding of the QHE is in the regime where there are no extended states at the Fermi level, so that dc transport, particularly the quantization of the Hall conductivity σ_{xy}, does not require knowledge of the scattering matrix.[2] Most properties, however, require a detailed understanding of the scattering process. These properties include the normal and Hall conductivities $\sigma_{\mu\nu}$ off of the quantized plateaus, at nonzero temperature or frequency, fluctuations and noise, and the entire nonlinear current-voltage characteristic.

Both classical and quantum scattering are considered here. The classical case is investigated because it is simpler and exact results are obtained that describe previously unsuspected complexity. The results have implications for higher Landau levels via the correspondence principle, and apply qualitatively to lower Landau levels as well.[3] Both smooth and abrupt scattering potentials (on the scale of the cyclotron orbit l, the magnetic length) are experimentally relevant in the QHE.[4] Smooth potentials ($|\nabla V|l \ll \hbar\omega_c$) are better behaved.[5] This paper concentrates on abrupt potentials. There is evidence that the qualitative features for abrupt potentials are *generic,* and apply to all potentials except those in the very smooth limit.

The Hamiltonian for an electron confined to the x-y plane in a uniform magnetic field $\mathbf{B}=\nabla\times\mathbf{A}=B\hat{\mathbf{z}}$ and Hall electric field $\mathbf{E}=E\hat{\mathbf{y}}$, with scattering potential $V(\mathbf{r})$, is

$$H=\frac{1}{2m^*}\left[\mathbf{p}-\frac{e\mathbf{A}}{c}\right]^2+eEy+V(\mathbf{r})\,. \tag{1}$$

If $V(\mathbf{r})$ changes discontinuously on a closed curve, the classical Hamiltonian flow can be represented by a two-dimensional map g. Successive collision points and collision angles are given by $(x_{j+1},\phi_{j+1})=g(x_j,\phi_j)$. Typical classical scattering dynamics is shown in Fig. 1(a). The particle generally makes several orbits around the scatterer. The center of the cyclotron orbit (guiding center) has a different final y coordinate than its initial y coordinate. Neither feature is found for smooth potentials.

One of the simplest scattering potentials is a hard finite horizontal wall (perpendicular to $\mathbf{E}$), with no thickness in the y direction. The horizontal wall is a *one-dimensional* Hamiltonian map (ϕ_j and the y guiding-center coordinate are constant). The perimeter is parametrized by $x\in[0,1]$ [Fig. 1(b)]. In these units the diameter of the cyclotron orbit is α, and the amount by which the orbit translates in one period, which is proportional to $\mathbf{E}$, is 2β. There is also an initial condition, the angle $\theta\in[0,2\pi]$ at which the particle begins with its guiding center a specified distance from the barrier. The guiding center has the same y coordinate as the barrier (a different y coordinate can be mapped onto a problem where y is the same).

A particle coming from $-\infty$ first collides in the interval $[0,2\beta]$, and makes its last collision on top in $I_1\equiv[\frac{1}{2}-\alpha-\beta,\frac{1}{2}]$. The particle escapes to $+\infty$ if it collides in the subinterval $[\frac{1}{2}-2\beta,\frac{1}{2}]$. Otherwise it wraps

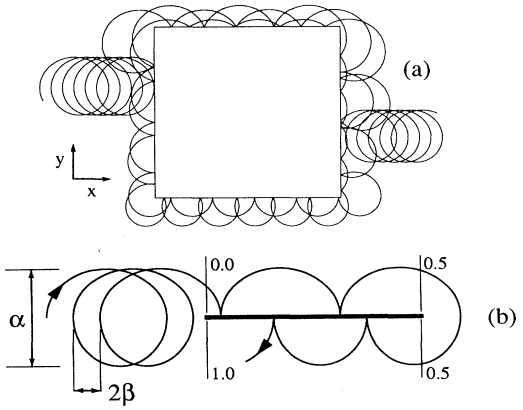

FIG. 1. The classical scattering of a charged particle from infinitely repulsive barriers calculated numerically for (a) a square barrier and (b) a horizontal wall.

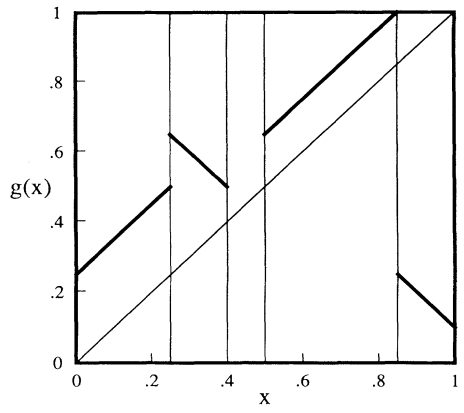

FIG. 2. The map $g(x)$ for $\alpha=0.2$ and $\beta=0.05$ is given by the heavy lines of slope ± 1. Points $x \in [0.4,0.5]$ escape.

around to the bottom [shown in Fig. 1(b)], and eventually wraps back to the top. The map $g(x)$ describing this physical scattering process is discontinuous, with slope everywhere ± 1 by Liouville's theorem (Fig. 2):

$$g(x)=\begin{cases} x+\alpha+\beta, & x \in [0, \frac{1}{2}-\alpha-\beta], \\ 1-x-2\beta, & x \in [\frac{1}{2}-\alpha-\beta, \frac{1}{2}-2\beta], \\ +\infty, & x \in [\frac{1}{2}-2\beta, \frac{1}{2}], \\ x+\alpha-\beta, & x \in [\frac{1}{2}, 1-\alpha+\beta], \\ 1-x+2\beta, & x \in [1-\alpha+\beta, 1]. \end{cases} \quad (2)$$

Attention is restricted to $\alpha+\beta<\frac{1}{2}$ and $0<\beta<\alpha$.

The number of collisions N can be calculated numerically as a function of $r \equiv \alpha+\beta$, $s \equiv \alpha-\beta$, and the initial angle θ. Figure 3 plots $N(r,s)$, the maximum number of collisions over all θ for a given (r,s), on a typical section. All peaks actually extend upward to infinity, and appear finite only because of numerical sampling. N contains infinite sets of divergences that accumulate at points such as $r=0.35$. Divergences result because infinite periodic trajectories exist. [A periodic trajectory resembles Fig. 1(b) with the incoming piece removed, and the trajectory on the bottom wrapping around to join the one on top.] One can prove, however, that a scattering state (one beginning at $-\infty$) can never be caught in a periodic trajectory. The divergences occur when the parameters are mistuned by an amount η from those resulting in exact periodicity. As $\eta \to 0$, one can show that long trajectories occur with $N \sim \eta^{-1}$, but that the initial θ must fall in an interval of $O(\eta)$ to become caught in a long trajectory. As shown below, there are also infinite *quasiperiodic* trajectories. The isolated divergences in Fig. 3 are trajectories that approach periodic orbits. The accumulation points are due to quasiperiodic orbits.

The set of points (r_∞, s_∞) in the two-dimensional parameter space at which infinite trajectories exist is displayed in Fig. 4. In spite of the set's complexity, most of it can be described analytically. An exact renormalization-group (RG) transformation is defined by the choice of a subinterval $[y_1,y_2] \in [0,1]$. The renormalized map $f=R(g)$ is the first return map on the subinterval [the first element of $g(x)$, $g(g(x))$, ... in the subinterval]. The initial subinterval is $I_1=[\frac{1}{2}-r, \frac{1}{2}]$. Figure 5 shows a return map f for I_1, rescaled to unit length. The interval I_1 is regarded as periodic (the points 0 and 1 are identified). The return map is a permutation of the adjacent intervals $[0,x_1]$ and $[x_1,x_2]$ followed by a rigid rotation, with points starting in $[x_2,1]$

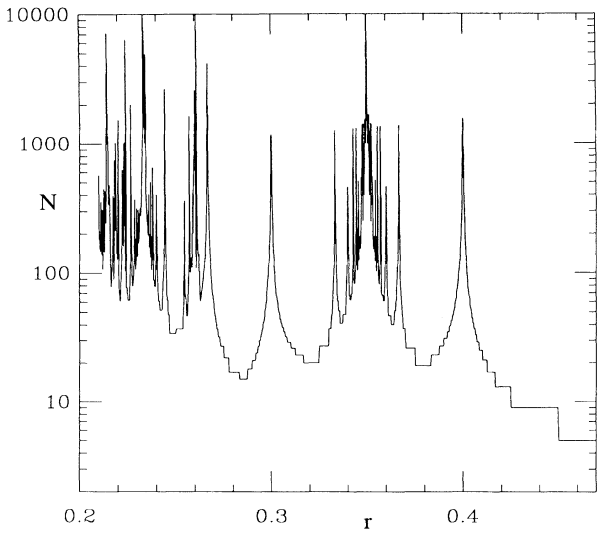

FIG. 3. The number of collisions $N(r,s)$ on a logarithmic scale as a function of r, with s fixed at 0.2.

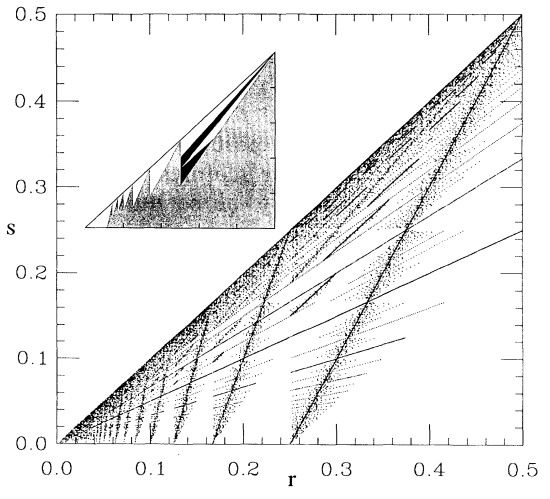

FIG. 4. Parameters at which infinite trajectories occur. All rational parameters of the form $(r,s)=(j_1/p, j_2/p)$, $p=2520$, are tested. Inset: the region P_1 (light shade), and part of P_2 (dark shade).

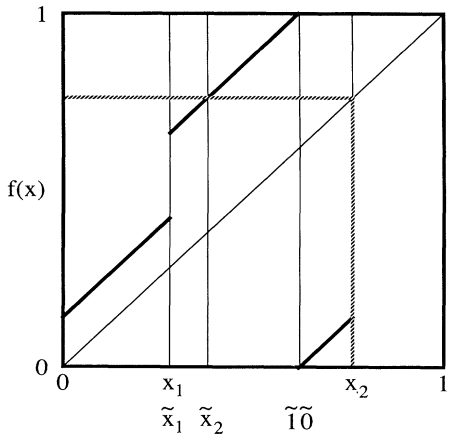

FIG. 5. A map $f(x)$ for the interval I_1 is given by the heavy lines of slope 1. Points in $[x_2,1]$ escape. The RG restricts the map to the subinterval $[0,x_2]$ (striped square). The subinterval is considered periodic, with $\tilde{0}\equiv\tilde{1}$. Escape from the subinterval occurs in $[\tilde{x}_2,\tilde{1}]$. The subinterval is then rotated so that $\tilde{0}$ is on the left, and lengths rescaled so that the new interval is one unit long.

escaping. The map f is characterized by three parameters, x_1, x_2, and δ_1, all between 0 and 1:

$$f(x)=\begin{cases}(x+\delta_1+x_2)\mathrm{mod}1, & x\in[0,x_1],\\ (x+\delta_1)\mathrm{mod}1, & x\in[x_1,x_2],\\ \infty, & x\in[x_2,1].\end{cases} \tag{3}$$

The initial parameters are $x_1^0=(s-\frac{1}{2}\ \mathrm{mod}s)/r$, $x_2^0=s/r$, and $\delta_1^0=(-x_1^0-1/2r-s/r)\mathrm{mod}1$.

The first renormalization is special in that it changes the nature of the map (compare Figs. 2 and 5). The successive renormalizations are defined by removing from the domain and range of $f(x)$ those points that immediately escape to infinity, leaving the interval $[0,x_2]$, as described in Fig. 5. The renormalized function is given by Eq. (3) with parameters x_1', x_2' and δ_1'. Using $y\equiv(x_1+\delta_1)\mathrm{mod}1$, one may show that the renormalized parameters are

$$x_1'=1+\frac{y-1}{x_2},\quad x_2'=2-\frac{1}{x_2}, \tag{4a}$$

if $1-x_2<y<x_2$,

$$x_1'=0,\quad x_2'=\min\left[1+\frac{y-1}{x_2},0\right], \tag{4b}$$

if $x_2\le y$,

$$x_1'=0,\quad x_2'=1-\frac{y}{x_2}, \tag{4c}$$

if $y\le 1-x_2$ and $y<x_2$,

$$\delta_1'=\frac{\delta_1}{x_2}, \tag{4d}$$

if $x_1<y<x_2$, and

$$\delta_1'=\frac{\delta_1-1}{x_2}\mathrm{mod}1, \tag{4e}$$

if $x_2\le y$ or $y\le x_1$.

The dynamics for any (r,s) is obtained by iteration of the renormalization group until it reaches one of its two fixed points. The first fixed point $(x_1,x_2)=(0,0)$ indicates that all trajectories escape to infinity. The second, $(x_1,x_2)=(0,1)$, describes a rigid rotation (with no escape or permutation) on the renormalized interval. An RG sequence that reaches the second fixed point indicates that (r,s) is such that there are trajectories that collide an infinite number of times with the barrier. Rational δ corresponds to periodic orbits, and irrational δ corresponds to quasiperiodic orbits.

An analytic solution can be given for the RG equations (4) when $x_1'=0$, so that the map describes rotation with escape, rather than permutation followed by rotation with escape. The parameter range P_1 in which the first renormalized map $R(f)$ is equivalent to rotation with escape is an infinite set of triangles, which is a large fraction of parameter space (Fig. 4, inset). In P_1, the escape width w and the rotation δ are given by

$$\begin{aligned}&w=\min[\rho-(1+1/2s)\mathrm{mod}\rho,1],\\ &\delta[1/2s+\rho-(1+1/2s)\mathrm{mod}\rho]\mathrm{mod}1,\end{aligned} \tag{5a}$$

if $\frac{1}{2}\ \mathrm{mod}r\le r-s$, and

$$\begin{aligned}&w=\min[(1+1/2s)\mathrm{mod}\rho,1],\\ &\delta[1/2s-(1+1/2s)\mathrm{mod}\rho]\mathrm{mod}1,\end{aligned} \tag{5b}$$

if $(\frac{1}{2}-r+s)\mathrm{mod}r<r-s$, where $\rho=r/s$. The analytic description of the set (r_∞,s_∞) in the region P_1 is given by (a) $w=0$, or (b) $\delta=p/q$ is rational, with p and q relatively prime, and $w<1/q$.[6] Case (a) corresponds to quasiperiodic orbits and (b) corresponds to periodic orbits. The set of all quasiperiodic orbits in P_1 may be written

$$(s+\tfrac{1}{2})\mathrm{mod}r=0. \tag{6}$$

One can analytically describe larger regions by defining P_2 in which $R(R(f))$ is rotation plus escape, etc. (Fig. 4). Quasiperiodic orbits along oblique lines [such as the one connecting (0.25,0) and (0.5,0.5)] impale periodic orbits occurring on rays from the origin. The extent of the periodic intervals is a discontinuous function of the ray angle.

The correspondence principle implies that the *quantum* dynamics of an electron in a high Landau level n will resemble the complex classical dynamics. Infinite trapping times need not exist as in the classical case, but long quantum trapping times and erratic phase shifts, diverging as $n\to\infty$, are expected. Preliminary numerical studies indicate that the qualitative aspects of the

classical dynamics apply to the low-Landau-level quantum case as well.[3] In particular, a wave packet splits at the far edge of a scattering potential, with part of its amplitude escaping to $+\infty$ and part recirculating around the potential. An electron can have a significant amplitude to scatter from an extended potential into a different Landau level (different y guiding center). Previous simulations were not in the correct regime to observe this effect.[7] The dynamics are due to high-order multiple scattering (some trajectories in Fig. 3 interact with the potential 10000 times), and are missed in single-scattering approximations like the self-consistent Born approximation.

If an electron encounters a succession of random scattering centers, the parameters vary for each scatterer. The number of collisions, and hence the waiting time near each scatterer, is a sensitive function of the parameters with a broad (power-law) distribution of waiting times (Fig. 3). This distribution typically results in $1/f$ noise.[8] Noise power with increasing amplitude at low frequencies has been experimentally observed in the quantum Hall regime.[9]

When the electron drift velocity exceeds a critical velocity v_c, it escapes from the upper edge of the scatterer, systematically emerging with a larger y guiding-center coordinate. This indicates the observed onset of σ_{xx} and breakdown of the QHE at high currents.[10] For a barrier of extent $L > l$ in the y direction, v_c is reached when the x guiding-center coordinate translates by more than a cyclotron radius l in the time required to reach the top of the barrier. The critical velocity is the order of $l^2\omega_c/L$, which is l/L smaller than the Zener tunneling estimate. The scatterer breaks translation invariance to allow tunneling to occur, and can cause tunneling to begin at a lower velocity than the Zener estimate, as observed in experiments.[10]

I would like to thank N. Nicopoulos, F. Waugh, S. Aubry, D. Farmer, M. Henon, A. Katz, and I. Satija for enlightening discussions. This work was supported by the U.S. DOE.

[1]For a review, see *The Quantum Hall Effect,* edited by R. E. Prange and S. M. Girvin (Springer-Verlag, New York, 1987).

[2]R. B. Laughlin, Phys. Rev. B **23**, 5632 (1981).

[3]Nikos Nicopoulos and S. A. Trugman, to be published.

[4]R. E. Prange, in Ref. 1, Chap. 3.

[5]S. A. Trugman, Phys. Rev. B **27**, 7539 (1983); R. E. Prange and R. Joynt, Phys. Rev. B **25**, 2943 (1982).

[6]R. L. Devaney, *An Introduction to Chaotic Dynamical Systems* (Addison-Wesley, Reading, MA, 1985).

[7]R. Joynt, J. Phys. C **17**, 4807 (1984); J. T. Chalker, J. Phys. C **16**, 4297 (1983).

[8]P. Dutta and P. M. Horn, Rev. Mod. Phys. **53**, 497 (1981).

[9]B. W. Ricketts, J. Phys. D **18**, 885 (1985); A. J. Kil *et al.*, Solid State Commun. **60**, 831 (1986).

[10]M. E. Cage *et al.*, Phys. Rev. Lett. **51**, 1374 (1983); H. L. Stormer *et al.*, in *Proceedings of the Seventeenth International Conference on the Physics of Semiconductors, San Francisco, 1984,* edited by J. D. Chadi and W. A. Harrison (Springer-Verlag, New York, 1985).

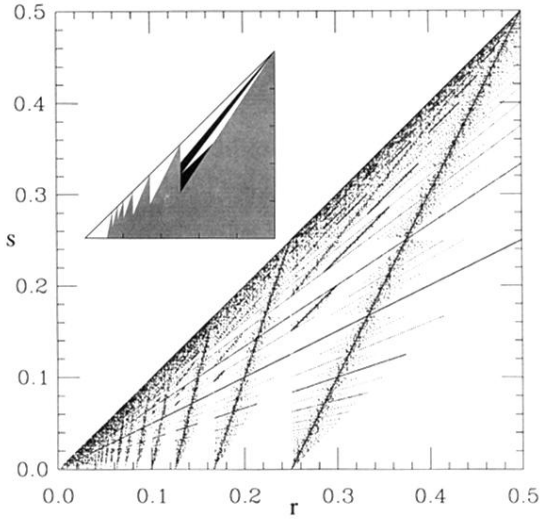

FIG. 4. Parameters at which infinite trajectories occur. All rational parameters of the form $(r,s)=(j_1/p,j_2/p)$, $p=2520$, are tested. Inset: the region P_1 (light shade), and part of P_2 (dark shade).